



HAL
open science

**Cu-Catalyzed P–C bond formation/cleavage:
straightforward synthesis/ring-expansion of strained
cyclic phosphoniums**

Maryne Duval, Charlie Blons, Sonia Mallet-Ladeira, Damien Delcroix, Lionel Magna, H  l  ne Olivier-Bourbigou, E. Daiann Sosa Carrizo, Karinne Miqueu, Abderrahmane Amgoune, Gy  rgy Szal  ki, et al.

► To cite this version:

Maryne Duval, Charlie Blons, Sonia Mallet-Ladeira, Damien Delcroix, Lionel Magna, et al.. Cu-Catalyzed P–C bond formation/cleavage: straightforward synthesis/ring-expansion of strained cyclic phosphoniums. Dalton Transactions, 2020, 49 (37), pp.13100-13109. 10.1039/d0dt03059g . hal-02970844v2

HAL Id: hal-02970844

<https://univ-pau.hal.science/hal-02970844v2>

Submitted on 13 Nov 2020

HAL is a multi-disciplinary open access archive for the deposit and dissemination of scientific research documents, whether they are published or not. The documents may come from teaching and research institutions in France or abroad, or from public or private research centers.

L'archive ouverte pluridisciplinaire **HAL**, est destinée au dépôt et à la diffusion de documents scientifiques de niveau recherche, publiés ou non, émanant des établissements d'enseignement et de recherche français ou étrangers, des laboratoires publics ou privés.

Cu-catalyzed P-C bond formation/cleavage: straightforward synthesis/ring-expansion of strained cyclic phosphoniums

Maryne Duval,^a Charlie Blons,^a Sonia Mallet-Ladeira,^b Damien Delcroix,^c Lionel Magna,^c H    ne Olivier-Bourbigou,^c E. Daiann Sosa Carrizo,^d Karinne Miqueu,^{*d} Abderrahmane Amgoune,^a Gy  rgy Szal  ki^a and Didier Bourissou^{*a}

^aCNRS/Universit   Toulouse III - Paul Sabatier, Laboratoire H  t  rochimie Fondamentale et Appliqu  e (LHFA, UMR 5069), 118 Route de Narbonne, 31062 Toulouse Cedex 09, France. E-mail: dbouriss@chimie.ups-tlse.fr

^bInstitut de Chimie de Toulouse (FR 2599), 118 Route de Narbonne, 31062 Toulouse Cedex 09, France.

^cIFP Energies nouvelles, Rond-Point de l'Echangeur de Solaize BP3, 69360 Solaize (France), France.

^dCNRS/Universit   de Pau et des Pays de l'Adour, Institut des Sciences Analytiques et Physico-Chimie pour l'Environnement et les Mat  riaux (IPREM, UMR 5254), H  lioparc, 2 Avenue du Pr  sident Angot, 64053 Pau Cedex 09, France. E-mail: kmiqueu@univ-pau.fr

Abstract:

Upon reaction with copper(I), *peri*-halo naphthyl phosphines readily form *peri*-bridged naphthyl phosphonium salts. The reaction works with alkyl, aryl and amino substituents at phosphorus, with iodine, bromine and chlorine as a halogen. It proceeds under mild conditions and is quantitative, despite the strain associated with the resulting 4-membered ring structure and the naphthalene framework. The transformation is amenable to catalysis. Under optimized conditions, the *peri*-iodo naphthyl phosphine **1-I** is converted into the corresponding *peri*-bridged naphthyl phosphonium salt **2b** in only 5 minutes at room temperature using 1 mol% of CuI. Based on DFT calculations, the reaction is proposed to involve a Cu(I)/Cu(III) cycle made of P-coordination, C–X oxidative addition and P–C reductive elimination. This copper-catalyzed route gives a general and efficient access to *peri*-bridged naphthyl phosphonium salts for the first time. Reactivity studies could thus be initiated and the possibility to insert gold into the strained P–C bond was demonstrated. It leads to (P,C)-cyclometallated gold(III) complexes. According to experimental observations and DFT calculations, two mechanistic pathways are operating: (i) direct oxidative addition of the strained P–C bond to gold, (ii) backward-formation of the *peri*-halo naphthyl phosphine (by C–P oxidative addition to copper followed by C–X reductive elimination), copper to gold exchange and oxidative addition of the C–X bond to gold. Detailed analysis of the reaction profiles computed theoretically gives more insight into the influence of the nature of the solvent and halogen atom, and provides rationale for the very different behaviour of copper and gold in this chemistry.

Introduction

Reductive elimination plays a pivotal role in organometallic chemistry. It intervenes in most catalytic cycles of transition-metal mediated cross-couplings as the key product-releasing step. Reductive coupling between L-type ligands (such as phosphines, thioethers, pyridines, *N*-heterocyclic carbenes...) and X-type groups (such as aryls, alkyls, halogens...) is also well-known (Figure 1). It has recently attracted an upsurge of interest, in particular the coupling of phosphines and aryl groups.¹⁻⁴ It is not only an efficient way to prepare aryl phosphonium salts (Figure 1, path a)⁵ but also an undesirable deactivation pathway for catalytic transformations involving phosphine-ligated aryl complexes. Aryl-aryl exchange between transition metals and phosphine ligands is also possible and this M–C/P–C bond metathesis process (Figure 1, path b) has been recently exploited to achieve catalytic functional group exchange between aryl chlorides and aryl iodides.⁶ In all this chemistry, the group 10 metals, Pd and Ni especially, occupy the forefront position due to their easy cycling between the M(0) and M(II) oxidation states.

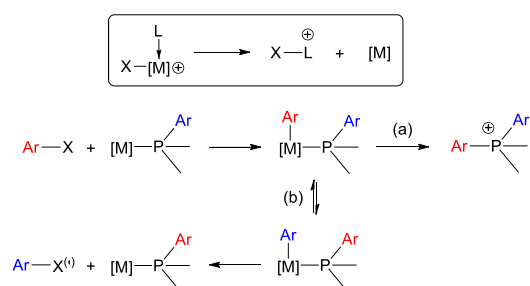


Figure 1. Top: Schematic representation of the reductive coupling between L and X-type ligands at transition metals. Bottom: Phosphine-aryl coupling promoted by transition metals (a) and aryl/aryl exchange between phosphines and transition metals (b).

Comparatively, much less is known in the field with the group 11 metals that are inherently reluctant to undergo oxidative addition and therefore to achieve 2-electron redox cycles. Examples of phosphine-aryl coupling at gold have become more numerous but are still rare.⁷ The formation of aryl phosphoniums has been authenticated as the favourite decomposition pathway of tricoordinate $[(R_3P)Au(Ar)X]^+$ complexes arising from oxidative addition of aryl halides to gold.⁸⁻¹¹ It has also been observed upon C–H activation of arenes at phosphine-ligated Au(III) complexes⁹ and by reacting (N,C)-cyclometallated Au(III) complexes with phosphines.¹²

The coupling of aryl groups and L ligands at copper is even scarcer.^{13,14} With phosphines, the only example we are aware of involves a bipyridine-functionalized bromo-arene (Figure 2a). Allen *et al.* tested other templated substrates, but this was the only one to undergo P–C coupling.¹⁵ A related coupling involving NHC instead of phosphine complexes was recently reported by Fairlamb, Ariarfarid and co-workers.¹⁶ Quantitative formation of a 2-arylated benzimidazolium salt was observed upon reaction with PhI (Figure 2b). Based on DFT calculations, the reaction was proposed to involve a Cu(I)/Cu(III) cycle (C–I oxidative addition, NHC–C reductive elimination). As pointed out by Huang *et al.* in their recent review,⁴ all the aryl-phosphine couplings described so far with the coinage metals require a stoichiometric amount of metal complex.¹⁷

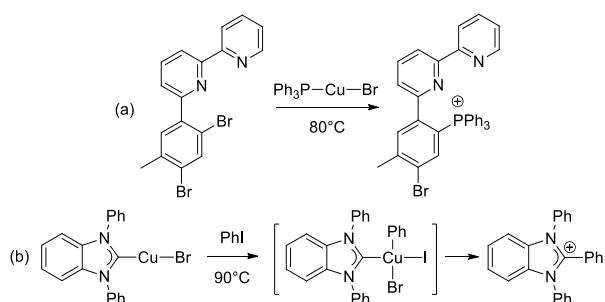
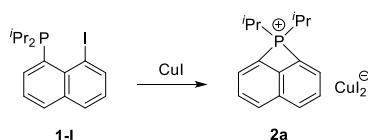


Figure 2. Copper-mediated couplings between L-type ligands and aryl groups.

In the course of our investigations of coinage metal complexes deriving from the *peri*-halo naphthyl phosphine such as **1-I**,^{18,19} we recently discovered an unexpected intramolecular P–C coupling leading to the *peri*-bridged naphthyl phosphonium salt **2a** (Scheme 1).²⁰ In this transformation, copper behaves very differently from gold which forms a (P,C)-cyclometallated complex.¹⁸



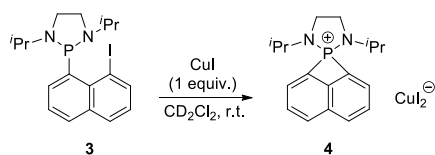
Scheme 1. Reaction of **1-I** with CuI: intramolecular phosphine–aryl coupling promoted by copper leading to a *peri*-bridged naphthyl-phosphonium **2a**.

Given the interest but very few P-*peri*-bridged naphthalenes²¹⁻²³ and the paucity of phosphine–aryl coupling at copper, we embarked in a comprehensive study of this process. This work is reported hereafter. Our aim was in particular to address the following questions: (i) is this transformation general? (ii) is it possible to make it catalytic? and (iii) what is the reactivity of the strained four-membered ring in such phosphoniums? The experimental study has been complemented by a thorough theoretical investigation to gain better understanding of the reaction mechanism and identify the underlying factors.

Results and Discussion

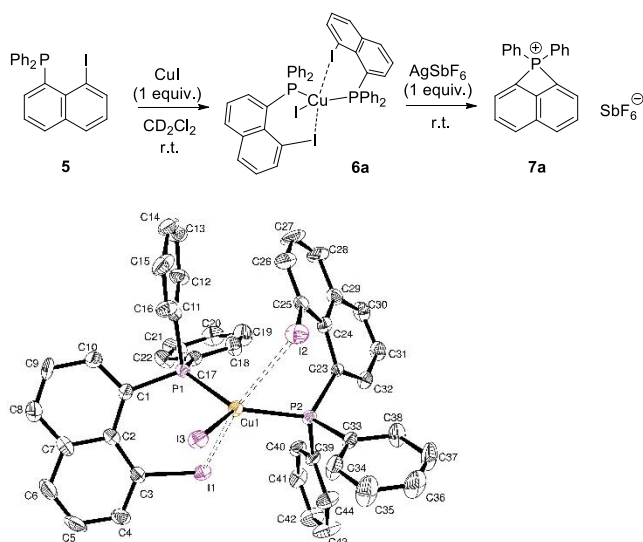
Variation of the substituents at phosphorus

The generality of the reaction was first examined by replacing the two *i*Pr groups at phosphorus by the diamino moiety (*i*Pr)NCH₂CH₂N(*i*Pr) that we have previously used in the context of *o*-carboranyl diphosphine ligands.²⁴ Upon reaction with CuI, the *peri*-iodo naphthylphosphine **3** readily formed the corresponding *spiro*-phosphonium **4**, which was characterized by multi-nuclear NMR spectroscopy (Scheme 2). Most characteristic is the symmetrisation of the naphthyl moiety, as apparent in the ¹H and ¹³C NMR spectra (Figures S1 and S2).²⁵



Scheme 2. Reaction of the diamino-substituted *peri*-iodo naphthyl phosphine **3** with CuI.

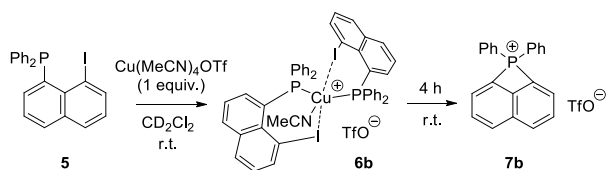
Then, we turned our attention to the phenyl-substituted phosphine **5**¹⁸ and observed a quite different behaviour (Scheme 3). Under similar conditions (CuI, dichloromethane, 25°C), a white precipitate formed rapidly. The corresponding ³¹P NMR signature (broad signal at δ -12.0 ppm) suggested in this case coordination of the phosphorus atom to copper, without formation of the phosphonium.²⁶ To shed light into the structure of the obtained product, an X-ray diffraction (XRD) analysis was carried out. It revealed, that **6a** is Cu(I) complex with two *peri*-iodo naphthyl phosphines coordinated to CuI. The copper atom sits in trigonal bipyramidal geometry [P–Cu–P = 130.58(6)°; sum of P–Cu–P and P–Cu–I bond angles = 359.66(5)° and is engaged in weak Cu⋯I contacts with the *peri*-iodine atoms located along the apical axis [3.037(9) and 3.319(10) Å, vs 2.575(8) Å for the equatorial CuI bond; I⋯Cu⋯I = 167.49(4)° (Table S3)].²⁷ Of note, the *peri*-I⋯Cu contacts induce significantly distortions of the naphthyl backbones, as apparent from the I–C⋯C–P torsion angles (–20.0(5) and 35.8(5)°).



Scheme 3. Reaction of the diphenyl-substituted *peri*-iodo naphthyl phosphine **5** with CuI and crystallographic structure of the ensuing bis-phosphine CuI complex **6a**.

To further analyze the weak Cu...I contacts observed crystallographically, DFT calculations were carried out on the actual complex **6a** using the B3PW91/SDD+f(Cu), SDD(I), 6-31G** level of theory (gas phase).²⁵ The optimized geometry nicely matches that determined experimentally by XRD (Table S6). In particular, the distances between Cu and the *peri*-I atoms are well reproduced (3.178 and 3.267 Å). In addition, NBO analysis confirms the presence of secondary I...Cu interactions, found as weak I(lone pair)→Cu(vacant 4s orbital) donor-acceptor interactions (Table S7) at the second-order perturbation theory analysis (the corresponding delocalization energies $\Delta E(2)$ amount to 12.7 and 10.0 kcal/mol, significantly less than that of the equatorial CuI bond, 77.3 kcal/mol).

Heating complex **6a** showed no evolution over time, even under forcing conditions (110°C for 2 days in toluene). Addition of AgSbF₆ was then tested to abstract iodide from copper and eventually favour oxidative addition of the C–I bond, as previously observed for the intramolecular activation of a Sn–Sn bond in diphosphine copper complexes.²⁸ Gratifyingly, the cyclic phosphonium **7a** rapidly and cleanly formed under these conditions. The thereby obtained SbF₆ salt was characterized by ¹H, ¹³C, ³¹P NMR spectroscopy, high-resolution mass spectrometry (in both positive and negative modes) as well as elemental analysis.²⁵ Notably, switching from CuI to Cu(MeCN)₄OTf as copper precursor circumvents the use of silver salt and offers a valuable alternative method to prepare phosphonium **7** (Scheme 4). Under these conditions, the diphosphine complex **6b** ($\delta^{31}\text{P}$ NMR: –7.5 ppm) forms instantaneously and then gradually evolves to the cyclic phosphonium **7b** within 4 hours at room temperature.



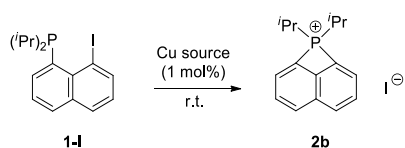
Scheme 4. Reaction of the diphenyl-substituted *peri*-iodo naphthyl phosphine **5** with Cu(MeCN)₄OTf.

From stoichiometric to catalytic transformations

The reaction conditions to access the *peri*-bridged naphthyl-phosphonium were then optimized using the isopropyl-substituted substrate **1-I**. Whatever the copper source employed, CuBr(SMe₂), Cu(MeCN)₄PF₆, Cu(MeCN)₄OTf or (Py)CuI, the formation of the phosphonium was instantaneous and quantitative at room temperature according to ³¹P NMR spectroscopy. Thus, neither the charge of the Cu precursor nor the ancillary ligands have a significant impact on the reaction. We then sought to decrease the loading in Cu source with the hope to develop a catalytic process. As mentioned above, all known examples of phosphine-aryl coupling at copper are stoichiometric. Pleasingly, complete and clean conversion of **1-I** into **2b** was observed using 20 mol% for (Py)CuI. The loading can even be decreased to 1 mol% with CuI and Cu(MeCN)₄OTf. To further optimize the transformation, different solvents were tested (Table 1). In general, polar solvents were preferred, due to solubility issues. Among those tested (DCM, MeCN, THF, DMF), the best results in terms of reaction rate, cleanness and isolation were obtained with THF and MeCN. In the end, two sets of conditions were established (entries 3 and 4). When using 1 mol% of Cu(MeCN)₄OTf in THF, the

reaction reached full conversion after 30 minutes at room temperature. The phosphonium **2b** precipitated in the course of its formation and was readily isolated (89% yield) by simple filtration. On the other hand, the phosphonium **2b** was obtained in only 5 minutes at rt by treating **1-I** with 1 mol% CuI in MeCN! Removal of MeCN and washing with THF resulted in a 91% isolated yield. Note that in both cases the phosphonium is obtained as its iodide salt **2b** containing *ca* 1 mol% of CuI₂⁻ counter-anion (the copper content, as determined by ICP-MS, corresponds to *ca* 1 mol%, in line with the introduced amount of catalyst).²⁵

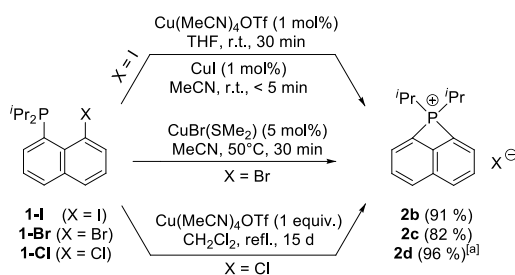
Table 1. Screening of the reaction conditions. Catalyst loading is 1 mol% for all entries. ^[a]Isolated yields in parentheses.



entry	Cu source	Solvent	Time	Conversion (%) ^[a]
1	Cu(MeCN) ₄ OTf	MeCN	60 min	100 (84)
2	Cu(MeCN) ₄ OTf	DMF	5 min	100
3	Cu(MeCN) ₄ OTf	THF	30 min	100 (89)
4	CuI	MeCN	5 min	100 (91)
5	CuI	THF	90 min	100

Generalization to *peri*-bromo and chloro-naphthyl phosphines

The possibility to extend this transformation of *peri*-iodo naphthyl-phosphines to the other halogens was then investigated. Different copper precursors and solvents were tested, the best results are disclosed in Scheme 5. Under stoichiometric conditions, the *peri*-bromo phosphine **1-Br** reacted a little slower than **1-I** (reaction is complete in 30 min instead of < 5 min in DCM at rt).²⁵ The transformation could nevertheless be efficiently achieved with catalytic amounts of copper. A protocol using 5 mol% of CuBr(SMe₂) and heating for 30 minutes at 50°C in MeCN was developed. The corresponding phosphonium salt **2c** was thereby isolated in 82% yield after work-up. The *peri*-chloro phosphine **1-Cl** was much more resilient to react. Heating for 15 days in refluxing DCM with 1 equiv. of Cu(MeCN)₄OTf was required. In this case, CuCl gradually precipitated and the phosphonium was obtained as the trifluoromethanesulfonate salt **2d** (as deduced from ESI in the negative mode) in 96% spectroscopic yield. Screening different reaction conditions by varying the copper precursor (CuCl), the solvent (MeCN, THF, *o*-DCB) and the temperature (80°C) did not lead to significant improvement.



Scheme 5. Optimized conditions for the Cu-mediated transformation of *peri*-halogenated naphthyl phosphines **1-X** into the corresponding *peri*-bridged naphthyl-phosponiums **2b-d**. ^[a]Yield based on ³¹P NMR spectroscopy.

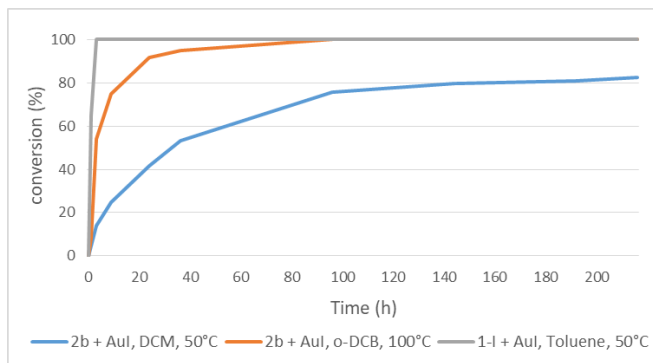
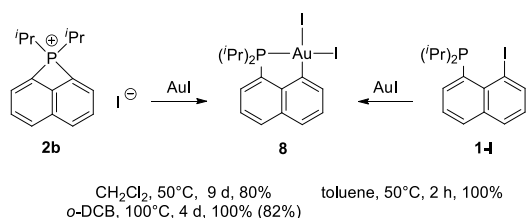
These results show that copper can activate not only the C–I bond but also C–Br and even the less reactive C–Cl bond of naphthyl-phosphines **1-X**. Catalytic transformations using low copper loadings were developed with **1-I** and **1-Br**, but with **1-Cl**, the reaction could not be driven to completion under catalytic conditions.

So far, only two *peri*-bridged naphthyl-phosponiums have been reported.^{21,22} They were prepared by a completely different route. *Peri*-bridged naphthyl-phosphines were first synthesized by intramolecular nucleophilic substitution at phosphorus. Then the phosphorus atom was quaternarized with methylating reagents. The copper-catalyzed route, as developed in this work, provides efficient and general access to such compounds. It gives the possibility to explore their reactivity, and our first investigations in this direction are described hereafter.

Ring-expansion of *peri*-bridged naphthyl-phosponiums

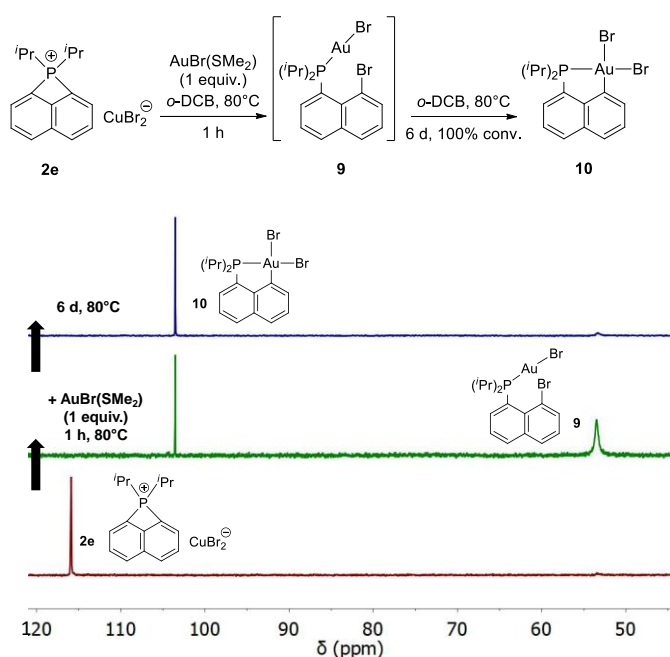
Peri-bridging imparts significant ring strain (as apparent from the acute bond angles CPC = 77° and PCC = 88°) and phosponiums such as **2** were thus supposed to be prone to ring-opening reactions. Our interest for gold complexes and unusual reactivity at gold²⁹ prompted us to explore the behaviour of phosponiums **2** towards Au(I) precursors. We were particularly intrigued by the possibility to insert gold into the P–C bond (*via* oxidative addition or any other pathway). Such a ring-expansion would lead to (P,C)-cyclometallated gold(III) species, complexes we have shown recently to display versatile reactivity^{19,30} and to be competent catalysts for the hydroarylation of alkynes.³¹

Pleasingly, the phosponium salt **2b** was found to react with gold(I) iodide to give the known (P,C)AuI₂ complex **8** (Scheme 6).^{19a} The reaction is significantly slower (80% spectroscopic yield after 9 d at 50°C) than when starting from the *peri*-iodo naphthyl phosphine **1-I** (100% in 2 h at 50°C). However, with phosponium **2b**, it does not benefit from P-coordination (and chelation assistance), and actually represents a rare example of intermolecular oxidative addition to gold. Performing the reaction in *ortho*-dichlorobenzene (*o*-DCB) at 100°C enabled to speed up the reaction (4 d, 82% isolated yield).



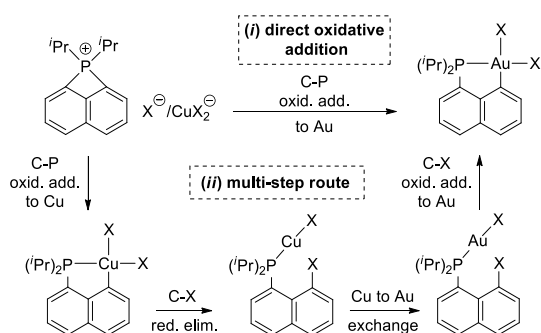
Scheme 6. Reactions of the *peri*-bridged naphthyl phosphonium **2b** with AuI (isolated yield in parentheses) and alternative synthesis of the ensuing (P,C)Au₂ complex **8** from **1-I**. Below: graph showing the rates of conversion of **2b/1-I** as determined by ³¹P NMR spectroscopy.

Then, the phosphonium salt **2e** deriving from the *peri*-bromo naphthyl phosphine **1-Br** was reacted with AuBr(SMe₂). NMR monitoring indicated complete consumption of the phosphonium **2e** after 1 h at 80°C with formation of a distinct intermediate displaying a ³¹P NMR resonance signal at δ 53.5 ppm (Scheme 7). The latter species was unambiguously assigned as the *peri*-bromo naphthyl phosphine gold(I) complex **9** that was also independently synthesized and fully characterized.^{18,25} From **9**, the (P,C)-cyclometallated gold(III) complex **10** formed gradually (complete conversion after 6 days at 80°C) by intramolecular oxidative addition of the C–Br bond to gold.



Scheme 7. Reaction of the *peri*-bridged phosphonium **2e** with AuBr(SMe₂) leading to the (P,C)-cyclometallated dibromo gold(III) complex **10**. Below: ³¹P NMR spectroscopic monitoring.

From a mechanistic standpoint, the formation of (P,C) cyclometallated gold(III) complexes upon reaction of the *peri*-bridged phosphonium with gold(I) iodide/bromide may be explained by the following pathways (Scheme 8): (i) direct oxidative addition of the strained P–C bond to gold, (ii) backward-formation of the *peri*-halo naphthyl phosphine (by C–P oxidative addition to copper followed by C–X reductive elimination), copper to gold exchange and oxidative addition of the C–X bond to gold. Of course, these two pathways may operate competitively or concomitantly.



Scheme 8. Schematic representation of the two possible pathways proposed to account for the formation of the cyclometallated gold(III) complexes (P,C)AuX₂ (X = I, Br).

We surmise that the direct oxidative route (i) prevails for the iodide salt **2b** which contains only trace amounts of copper (as CuI₂[−] counter-anion). No intermediate is detected during the course of the reaction in this case. As mentioned above, intermolecular oxidative addition to gold is rare, but not unprecedented. In particular, a few examples have been reported with strained C–C bonds as those of biphenylene and benzocyclobutanone.^{32,33} The reaction of Pt(PPh₃)₄ with a W(CO)₅-coordinated *peri*-bridged naphthyl phosphine, as described by Mizuta and Miyoshi, also deserves to be mentioned here.^{21a,b} Oxidative addition of the P–C bond to Pt induced ring-expansion and afforded original heterodinuclear complexes.

In the case of the CuBr₂[−] salt **2e**, the reaction seems to operate by the multi-step route (ii) instead. This is apparent from the characterization of the phosphine Au(I) complex **9**. Of note, the back-formation of the *peri*-bromo phosphine from **2e** demonstrates the reversibility of the C–Br oxidative addition / P–C reductive elimination sequence at copper.

The experimental work was paralleled with a thorough computational study, with the aim (i) to shed light into the mechanism of formation of the *peri*-bridged phosphonium mediated by copper and identify the factors influencing it (solvent, halogen), (ii) to rationalize the difference observed between copper and gold, and (iii) to gain more insight into the P–C bond cleavage and ring-expansion upon reaction with gold(I) halides.

Mechanism of formation of the *peri*-bridged naphthyl phosphonium mediated by copper

Previous DFT calculations performed in the gas phase supported the 2e redox sequence made of P coordination, C–I oxidative addition and P–C reductive elimination as a viable process for the reaction of the *peri*-iodo naphthyl phosphine **1-I** with CuI. To describe and analyze more reliably the experimental observations, solvent effects were taken into account, considering both DCM ($\epsilon = 8.93$) and MeCN ($\epsilon = 35.69$) using the universal Solvation Model based on solute electron Density (SMD). The corresponding energy profiles are given in Figure 3 (see also Figures S18 and S19).²⁵ Once the phosphine is coordinated to copper, oxidative addition of the C–I bond proceeds *via* a 3-centered transition state **TS1** (Figure 4a). This step is very mildly affected by the reaction conditions. In all cases, it is about thermoneutral (2.7, 1.9 and –1.4 kcal/mol in the gas phase, DCM and MeCN) and its activation barrier is low (9.3, 9.5 and 7.8 kcal/mol, respectively). More pronounced differences were found on the P–C coupling step following the (P,C)Cu(III)I₂ intermediate **II**, in line with the high polarity of the corresponding transition state **TS2** (Figure 4b) and resulting product. From **II**, the formation of the phosphonium salt **2** is only slightly downhill in energy in the gas phase (–1.9 kcal/mol), but well favoured thermodynamically in DCM (ΔG –14.2 kcal/mol) and MeCN (ΔG –13.7 kcal/mol). The overall transformation is thermoneutral in the gas phase (0.8 kcal/mol) but noticeably exergonic in DCM (–12.3 kcal/mol) and MeCN (–15.1 kcal/mol). Of note, the energy barrier for the reductive elimination at copper is significantly reduced with polar solvents: from 18.5 kcal/mol in the gas phase, it decreases to 7.6 kcal/mol in DCM, and to 6.3 kcal/mol in MeCN. Overall, the energy span for this Cu(I)/Cu(III) sequence is remarkably small. The activation barriers for the C–I oxidative addition and P–C reductive elimination are both under 10 kcal/mol, in line with the very fast reaction observed experimentally between **1-I** and CuI at room temperature even under catalytic conditions. It is noteworthy that the cleavage of the C–I bond is slightly more demanding than the formation of the P–C bond (by 1.5 to 1.9 kcal/mol), making the copper(III) complex **II** a fleeting intermediate.³⁴ This is consistent with the fact that no other complex than the starting phosphine Cu(I) species was observed experimentally.

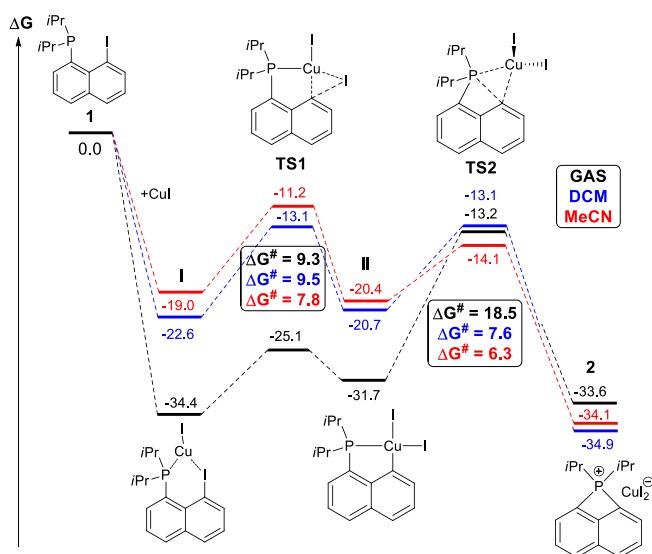


Figure 3. Energy profiles computed in the gas phase and in DCM/MeCN solutions for the C–I oxidative addition / P–C reductive elimination sequence. Free energies in kcal/mol computed at

GAS-B3PW91/SDD+f(Cu),SDD(I),6-31G**(other atoms) and SMD(DCM or MeCN)-B3PW91/SDD+f(Cu),SDD(I),6-31G**(other atoms) levels of theory.

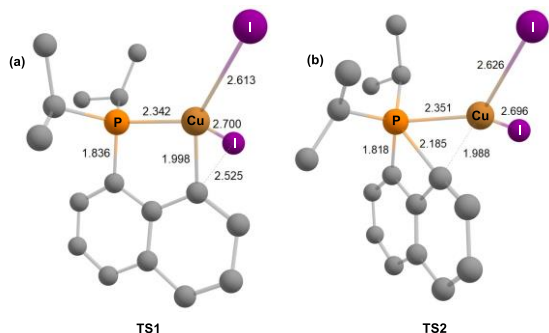


Figure 4. Transition states **TS1** and **TS2** computed respectively for the C–I oxidative addition **(a)** and P–C reductive elimination **(b)** at the SMD(DCM)-B3PW91/SDD+f(Cu),SDD(I),6-31G**(other atoms) level of theory. Key distances in Å.

Comparison of the *peri*-iodo, bromo and chloro naphthyl phosphines **1-X**

The influence of the halogen atom in the *peri*-position of the naphthyl-phosphine was then investigated. The energy profiles for the sequence of P-coordination, C–X oxidative addition to Cu and P–C reductive elimination were computed at the SMD(MeCN)-B3PW91/SDD+f(Cu),SDD(I,Br,Cl),6-31G**(other atoms) level of theory for the reactions **1-I** + CuI, **1-Br** + CuBr and **1-Cl** + CuCl in MeCN. The barrier for the oxidative addition to Cu increases progressively in the series C–I < C–Br < C–Cl (7.8, 13.7 and 18.5 kcal/mol) (Figure 5, see also Figures S20–S22)²⁵ and this step is less favoured thermodynamically for chlorine and bromine than for iodine (–1.4 for I *versus* 3.1 for Br and 1.8 kcal/mol for Cl). The halogen is not directly involved in the following P–C bond formation and has logically less impact on this step. In all cases, the reductive elimination is downhill in energy, by 13.7 kcal/mol for I, 16.2 kcal/mol for Br and 10.3 kcal/mol for Cl, over the (P,C)-cyclometallated Cu(III) complex **II**. The corresponding energy barrier increases from iodine (6.3 kcal/mol) to bromine (9.5 kcal/mol), and chlorine (12.8 kcal/mol). Overall, the formation of the phosphonium salts from **1-X** + CuX is thermodynamically favoured and the energy balance does not change much with the halogen ($\Delta G = -15.1$ kcal/mol for I, -13.1 kcal/mol for Br and -8.5 kcal/mol for Cl).³⁵ While the activation barriers for the C–X oxidative addition and P–C reductive elimination are close for iodine, the first step is significantly more demanding for bromine and chlorine (by 4.2 and 5.7 kcal/mol, respectively), making it the likely rate-determining step.

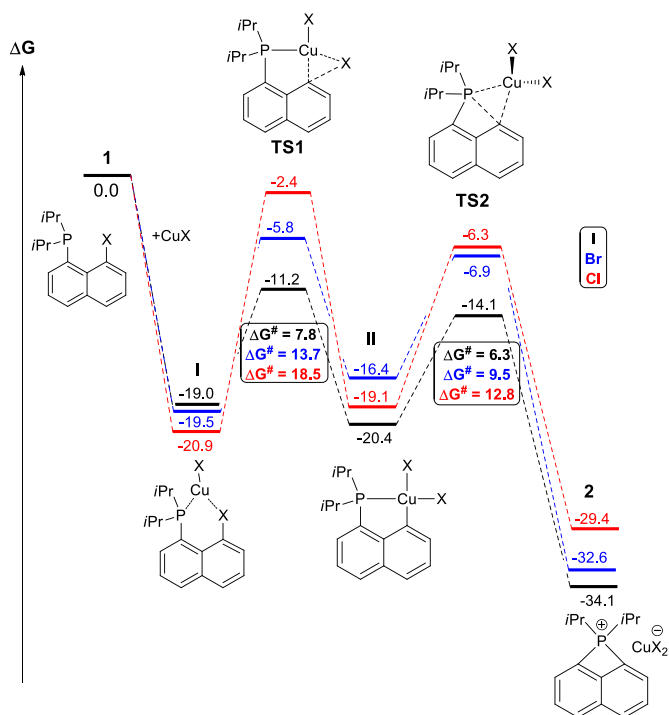


Figure 5. Energy profiles computed for the C–X oxidative addition (X : I, Br, Cl) / P–C reductive elimination sequence at the SMD(CH₃CN)-B3PW91/SDD+f(M),SDD(I,Br,Cl), 6-31G**(other atoms) level of theory. Free energies in kcal/mol.

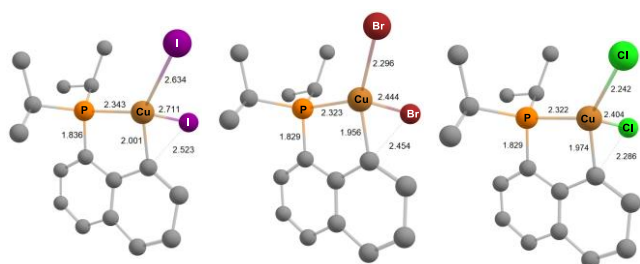


Figure 6. Transition states (TS1) computed for the C–I, C–Br and C–Cl oxidative additions to copper at the SMD(MeCN)-B3PW91/SDD+f(Cu),SDD(I,Br,Cl),6-31G**(other atoms) level of theory. Key distances in Å.

Comparison of copper and gold: formation and ring-expansion of the *peri*-bridged naphthyl phosphonium

Finally, we sought to better understand the very different behaviour exhibited by copper and gold, *ie* the formation of *peri*-bridged naphthyl phosphoniums with Cu *versus* (P,C)-cyclometallated gold(III) complexes with Au. Computations were carried out in DCM to enable comparison between the two metals under similar conditions used experimentally. The reaction profiles computed for the reactions of **1-I** with AuI and CuI are overlaid in Figure 7, revealing striking differences.

Consistent with experimental observations,^{18,36} the reaction stops at the $M(III)I_2$ stage with gold: the P–C reductive elimination leading to the phosphonium is uphill in energy (+ 7.8 kcal/mol) and its activation barrier is large (38.1 kcal/mol). Conversely, starting from the AuI_2^- phosphonium **2**, oxidative addition of the strained P–C bond to give the (P,C) AuI_2 complex **II** is downhill in energy. The corresponding barrier (30.3 kcal/mol) is significantly larger than that of the P-assisted C–I oxidative addition from **I** (16.6 kcal/mol), but can be crossed over at high temperature, in line with that observed experimentally.

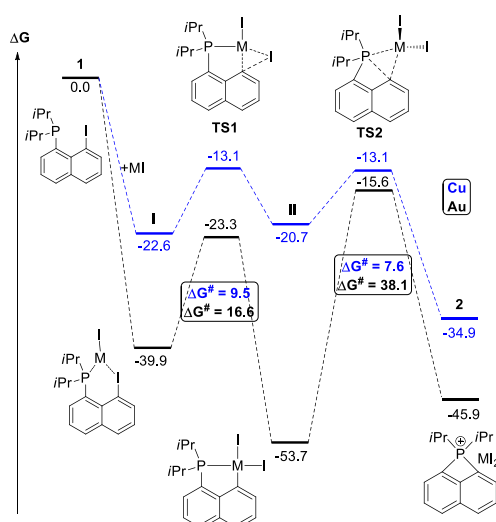


Figure 7. Overlay of the energy profiles computed for the reactions of the *peri*-iodo naphthyl phosphine **1-I** with CuI and AuI at the SMD(DCM) B3PW91/SDD+f(M),SDD(I),6-31G**(other atoms) level of theory. Free energies in kcal/mol.

The formation of the $M(III)I_2$ species **II** is less favoured thermodynamically with copper than gold, consistent with their intrinsic properties and relativistic effects.³⁷ Due to the smaller size of Cu compared to Au, the (P,C)-cyclometallated structure imposes some geometric constraint, but not too much (Figure 8). Of note, the barrier for C–I oxidative addition is lower for copper than for gold (9.5 *versus* 16.6 kcal/mol). This has probably to do with the structure of the phosphine $M(I)$ precursor **I**, which is the standard situation for Au, but a low coordinate state for copper.³⁸

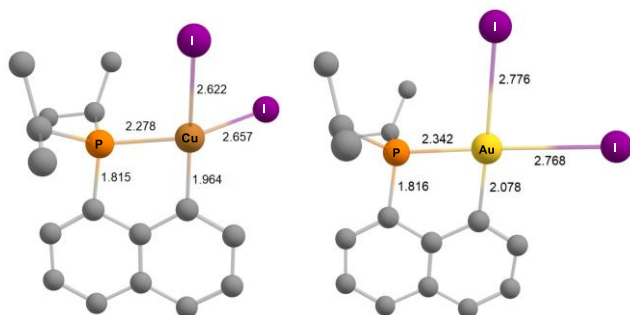


Figure 8. Structures computed for the (P,C)-cyclometallated $M(III)$ complexes **II** ($M = Cu, Au$) at the SMD(DCM)-B3PW91/SDD+f(M),SDD(I),6-31G**(other atoms) level of theory. Key distances in Å.

The same trend is observed from **1-Br** (Figure 9). As mentioned above, the activation barriers for C–Br oxidative addition to copper and P–C reductive elimination are both readily accessible (13.9 and 11.0 kcal/mol, respectively), and the formation of the *peri*-bridged phosphonium **2** is thermodynamically favoured over the (P,C)-cyclometallated Cu(III) complex **II** (ΔG° : –12.5 kcal/mol). Comparatively, the reaction with AuBr stops at the oxidative addition stage, the (P,C)Au(III)Br₂ complex is in a thermodynamic sink.

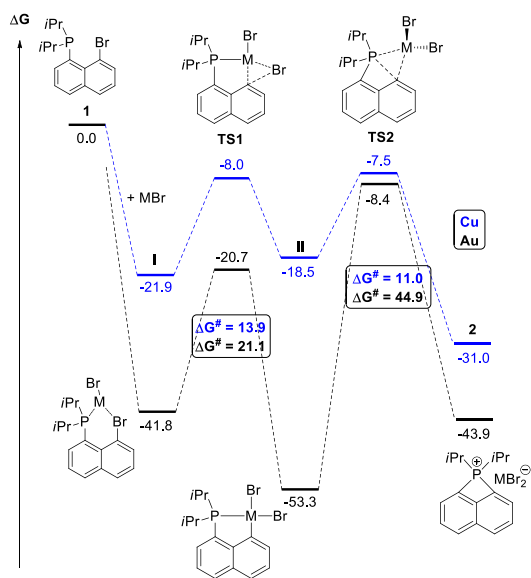


Figure 9. Overlay of the energy profiles computed for the reaction of the *peri*-bromo naphthyl phosphine **1-Br** with CuBr and AuBr at the SMD(DCM)-B3PW91/SDD+f(M),SDD(Br),6-31G** (other atoms) level of theory. Free energies in kcal/mol.

It is 11.5 kcal/mol lower in energy than the phosphine Au(I)Br complex **I** and 9.4 kcal/mol lower in energy than the *peri*-bridged phosphonium **2**. The activation barrier for P–C reductive elimination is very large (44.9 kcal/mol). Even that for the backward reaction, the oxidative addition of the strained P–C_{sp2} bond to gold (35.5 kcal/mol) is very high.

This is probably why the reaction of **2** with AuBr goes through the phosphine complex (**1-Br**)Au(I)Br and is mediated by copper. Insertion of CuBr₂[–] in the strained cyclic phosphonium is much less energy demanding than that of AuBr₂[–] (ΔG° 23.5 kcal/mol for the P–C oxidative addition to Cu). From **II**, C–Br reductive elimination is also facile at Cu (ΔG° 10.5 kcal/mol) and reforms the *peri*-bromo naphthyl phosphine.

The energy landscapes computed for Cu and Au are very different. The formation of the (P,C)-cyclometallated gold(III) complex is a strong driving force while the small energy span of the 2e redox sequence at copper explains its ease and reversibility.

Conclusion

In summary, the reaction of *peri*-halo naphthyl phosphines with Cu(I) was found not to stop after P-coordination and oxidative addition of the C–X bond as for gold. P–C reductive elimination readily proceeds to give strained *peri*-bridged naphthyl phosphonium salts. The reaction is general, as shown by the formation of the diamino-substituted, *spiro*-bicyclic phosphonium **4** and diphenyl-substituted phosphonium **7** (for which a bis-phosphine copper(I) complex featuring weak contacts between copper and the *peri*-iodine atoms was authenticated crystallographically). Not only naphthyl phosphines featuring C–I bonds in *peri* position react with copper(I) salts to give phosphoniums, but also the bromo and chloro derivatives **1-Br** and **1-Cl** although more forcing conditions are required. Remarkably, the reaction is amenable to catalysis and actually stands as the first Cu-catalyzed phosphine-aryl coupling. With the *peri*-iodo naphthyl phosphine **1-I**, it proceeds very fast under mild conditions (5 minutes at room temperature) with only 1 mol% of copper source.

The reaction most likely involves a Cu(I)/Cu(III) cycle made of P-coordination, C–X oxidative addition and P–C reductive elimination, as supported by DFT calculations. In line with experimental observations, polar solvents such as DCM and MeCN are preferred. They make the formation of the phosphonium salt more thermodynamically favourable and lower the activation barrier for the P–C reductive elimination step. The energy span for the Cu(I)/Cu(III) sequence is remarkably small, with activation barriers for C–I oxidative addition and P–C reductive elimination both under 10 kcal/mol. The influence of the halogen atom (I, Br, Cl) was also examined computationally. Accordingly, C–X oxidative addition is more demanding with bromine and chlorine, and represents the rate-determining step. The reaction profiles computed for gold are very different, explaining the striking difference observed between the two metals experimentally. The (P,C)-cyclometallated Au(III)X₂ complexes are in thermodynamic sinks. With gold, P–C reduction elimination is uphill in energy and its activation barrier is very high.

Because of the strain induced by the four-membered ring structure and the rigid naphthyl backbone, *peri*-bridged naphthyl phosphonium salts can be expected to be quite reactive. First studies in this direction have shown the possibility of ring-expansion by reaction of gold(I) precursors, leading to (P,C)-cyclometallated gold(III) complexes. Mechanistic studies have evidenced two contributing scenarios in which the insertion of the gold atom into the strained P–C bond proceeds either directly by oxidative addition to gold or involves the reversibility of the Cu(I)/Cu(III) sequence and ultimately oxidative addition of the C–X bond to gold assisted by P-chelation.

Peri-bridged naphthyl phosphonium salts represent a new type of π -conjugated phosphoniums, besides phospholium, benzophospholium and phosphaphenalium salts.³⁹ Future work will aim at exploring further their chemistry and studying related *peri*-P-bridged naphthyl compounds. Besides their reactivity, their photophysical properties certainly deserve to be investigated. Indeed, the incorporation of main-group elements in π -extended systems has been established as a very powerful strategy to alter their electronic and optical properties.⁴⁰

Acknowledgments

This work was supported financially by the Centre National de la Recherche Scientifique, the Université Toulouse III – Paul Sabatier and IFP Energies nouvelles. The "Direction du Numérique" of the Université de Pau et des Pays de l'Adour, MCIA (Mésocentre de Calcul Intensif Aquitain) and CINES under allocation A007080045 made by Grand Equipement National de Calcul Intensif (GENCI)

are acknowledged for computational facilities. E.D.S.C. thanks CDAPP for funding part of his post-doctoral contract.

References

1. S. A. Macgregor, *Chem. Soc. Rev.*, 2007, **36**, 67.
2. Y. H. Lee and B. Morandi, *Coord. Chem. Rev.*, 2019, **386**, 96.
3. L. Wang, H. Chen and Z. Duan, *Chem.–Asian J.*, 2018, **13**, 2164.
4. T. Jiang, H. Zhang, Y. Ding, S. Zou, R. Chang and H. Huang, *Chem. Soc. Rev.*, 2020, **49**, 1487.
5. (a) D. Marcoux and A. B. Charette, *J. Org. Chem.*, 2008, **73**, 590; (b) D. Marcoux and A. B. Charette, *Adv. Synth. Catal.*, 2008, **350**, 2967.
6. Y. H. Lee and B. Morandi, *Nat. Chem.*, 2018, **10**, 1016.
7. For C–P coupling reactions catalyzed by gold, see: (a) Y. He, H. Wu and F. D. Toste, *Chem. Sci.*, 2015, **6**, 1194; (b) H. Peng, R. Cai, C. Xu, H. Chen and X. Shi, *Chem. Sci.*, 2016, **7**, 6190.
8. For an early study in the gas phase, see: P. S. D. Robinson, G. N. Khairallah, G. da Silva, H. Lioe and R. A. J. O'Hair, *Angew. Chem. Int. Ed.*, 2012, **51**, 3812.
9. For the formation of tricoordinate $[(R_3P)Au(Ar)X]^+$ complexes by halide abstraction using silver salts, see: H. Kawai, W. J. Wolf, A. G. DiPasquale, M. S. Winston and F. D. Toste, *J. Am. Chem. Soc.*, 2016, **138**, 587.
10. For aryl-phosphine coupling at copper promoted by supramolecular cages, see: T. A. Bender, M. Morimoto, R. G. Bergman, K. N. Raymond and F. D. Toste, *J. Am. Chem. Soc.*, 2019, **141**, 1701.
11. For the detection of aryl-phosphoniums as side-products in gold-catalyzed transformations, see: (a) X.-z. Shu, M. Zhang, Y. He, H. Frei and F. D. Toste, *J. Am. Chem. Soc.*, 2014, **136**, 5844; (b) V. Gauchot and A.-L. Lee, *Chem. Commun.*, 2016, **52**, 10163; (c) V. Gauchot, D. R. Sutherland and A. L. Lee, *Chem. Sci.*, 2017, **8**, 2885; (d) B. Dong, H. Peng, S. E. Motika and X. Shi, *Chem.–Eur. J.*, 2017, **23**, 11093.
12. R. Bonsignore, S. R. Thomas, W. T. Klooster, S. J. Coles, R. L. Jenkins, D. Bourissou, G. Barone and A. Casini, *Chem.–Eur. J.*, 2020, **26**, 4226.
13. (a) M. Font, T. Parella, M. Costas and X. Ribas, *Organometallics*, 2012, **31**, 7976; (b) A. Casitas and X. Ribas, *Chem. Sci.*, 2013, **4**, 2301; (c) L. Liu and Z. Xi, *Chin. J. Chem.*, 2018, **36**, 1213.
14. For reviews dealing with Cu-catalyzed C–P coupling reactions, see: (a) I. P. Beletskaya and A. V. Cheprakov, *Coord. Chem. Rev.*, 2004, **248**, 2337; (b) H. Zhang, X.-Y. Zhang, D.-Q. Dong and Z.-L. Wang, *RSC Adv.*, 2015, **5**, 52824.
15. D. W. Allen, P. E. Cropper and I. W. Nowell, *Polyhedron*, 1989, **8**, 1039.
16. (a) T. J. Williams, J. T. W. Bray, B. R. M. Lake, C. E. Willans, N. A. Rajabi, A. Ariaferd, C. Manzini, F. Bellina, A. C. Whitwood and I. J. S. Fairlamb, *Organometallics*, 2015, **34**, 3497; (b) Y. Younesi, B. Nasiri, R. BabaAhmadi, C. E. Willans, I. J. S. Fairlamb, A. Ariaferd, *Chem. Commun.*, 2016, **52**, 5057.
17. For the C–H arylation of (benz)imidazolium salts with aryl iodides using 20 mol% of Cu_2O , see: S. Li, J. Tang, Y. Zhao, R. Jiang, T. Wang, G. Gao and J. You, *Chem. Commun.*, 2017, **53**, 3489.
18. J. Guenther, S. Mallet-Ladeira, L. Estevez, K. Miqueu, A. Amgoune and D. Bourissou, *J. Am. Chem. Soc.*, 2014, **136**, 1778.
19. (a) F. Rekhroukh, R. Brousses, A. Amgoune and D. Bourissou, *Angew. Chem. Int. Ed.*, 2015, **54**, 1266; (b) F. Rekhroukh, L. Estevez, S. Mallet-Ladeira, K. Miqueu, A. Amgoune and D. Bourissou, *J. Am. Chem. Soc.*, 2016, **138**, 11920; (c) F. Rekhroukh, L. Estevez, C. Bijani, K. Miqueu, A. Amgoune and D. Bourissou, *Organometallics*, 2016, **35**, 995.
20. C. Blons, M. Duval, D. Delcroix, H. Olivier-Bourbigou, S. Mallet-Ladeira, E. D. Sosa Carrizo, K. Miqueu, A. Amgoune and D. Bourissou, *Chem.–Eur. J.*, 2018, **24**, 11922.
21. (a) T. Mizuta, T. Nakazono and K. Miyoshi, *Angew. Chem. Int. Ed.*, 2002, **41**, 3897; (b) T. Mizuta, Y. Iwakuni, T. Nakazono, K. Kubo and K. Miyoshi, *J. Organomet. Chem.*, 2007, **692**, 184; (c) T. Mizuta, N. Tanaka, Y. Iwakuni, K. Kubo and K. Miyoshi, *Organometallics*, 2009, **28**, 2808.
22. P. Wawrzyniak, A. M. Z. Slawin, A. L. Fuller, J. D. Woollins and P. Kilian, *Dalton Trans.*, 2009, 7883.
23. A *peri*-bridged naphthyl phosphonium has been proposed as a transient intermediate in the reaction of 1,8-bis(diphenylphosphino)naphthalene with 1,8-bis(bromomethyl)-naphthalene, see: K. Owsianik, L. Vendier, J. Błaszczuk and L. Sieroń, *Tetrahedron*, 2013, **69**, 1628.
24. (a) M. Joost, A. Zeineddine, L. Estévez, S. Mallet-Ladeira, K. Miqueu, A. Amgoune and D. Bourissou, *J. Am. Chem. Soc.*, 2014, **136**, 14654; (b) M. Joost, L. Estévez, S. Mallet-Ladeira, K. Miqueu, A. Amgoune and D. Bourissou, *Angew. Chem. Int. Ed.*, 2014, **53**, 14512; (c) A. Zeineddine, F. Rekhroukh, E. D. Sosa Carrizo, S. Mallet-Ladeira, K. Miqueu, A. Amgoune and D. Bourissou, *Angew. Chem. Int. Ed.*, 2018, **57**, 1306.
25. See the ESI for details.[†]
26. P. F. Barron, J. C. Dyason, P. C. Healy, L. M. Engelhardt, C. Pakawatchai, V. A. Patrick and A. H. White, *Dalton Trans.*, 1987, 1099.
27. For structurally characterized bis(phosphine)CuX complexes, see for examples: (a) H. Kaddouri, V. Vicente, A. Ouali, F. Ouazzani and M. Taillefer, *Angew. Chem. Int. Ed.*, 2009, **48**, 333; (b) S. K. Gibbons, R. P. Hughes, D. S. Glueck, A. T. Royappa, A. L. Rheingold, R. B. Arthur, A. D. Nicholas and H. H. Patterson, *Inorg. Chem.*, 2017, **56**, 12809.
28. N. Lassauque, P. Gualco, S. Mallet-Ladeira, K. Miqueu, A. Amgoune and D. Bourissou, *J. Am. Chem. Soc.*, 2013, **135**, 13827.
29. M. Joost, A. Amgoune and D. Bourissou, *Angew. Chem. Int. Ed.*, 2015, **54**, 15022.
30. (a) F. Rekhroukh, L. Estévez, C. Bijani, K. Miqueu, A. Amgoune and D. Bourissou, *Angew. Chem. Int. Ed.*, 2016, **55**, 3414; (b) F. Rekhroukh, C. Blons, L. Estevez, S. Mallet-Ladeira, K. Miqueu, A. Amgoune and D. Bourissou, *Chem. Sci.*, 2017,

- 8, 4539; (c) A. Pujol, M. Lafage, F. Rekhroukh, N. Saffon-Merceron, A. Amgoune, D. Bourissou, N. Nebra, M. Fustier-Boutignon and N. Mézailles, *Angew. Chem. Int. Ed.*, 2017, **56**, 12264.
31. C. Blons, S. Mallet-Ladeira, A. Amgoune and D. Bourissou, *Angew. Chem. Int. Ed.*, 2018, **57**, 11732.
32. (a) C.-Y. Wu, T. Horibe, C. B. Jacobsen and F. D. Toste, *Nature*, 2015, **517**, 449–454; (b) M. Joost, L. Estévez, K. Miqueu, A. Amgoune and D. Bourissou, *Angew. Chem. Int. Ed.*, 2015, **54**, 5236; (c) J. Chu, D. Munz, R. Jazzar, M. Melaimi and G. Bertrand, *J. Am. Chem. Soc.*, 2016, **138**, 7884.
33. J. H. Teles, *Angew. Chem. Int. Ed.*, 2015, **54**, 5556.
34. Stable organocopper(III) species have been prepared using macrocyclic *N*-containing ligands: (a) H. Furuta, H. Maeda and A. Osuka, *J. Am. Chem. Soc.*, 2000, **122**, 803; (b) Y. K. Maurya, K. Noda, K. Yamasumi, S. Mori, T. Uchiyama, K. Kamitani, T. Hirai, K. Ninomiya, M. Nishibori, Y. Hori, Y. Shiota, K. Yoshizawa, M. Ishida and H. Furuta, *J. Am. Chem. Soc.*, 2018, **140**, 6883; (c) X. Ribas, D. A. Jackson, B. Donnadieu, J. Mahía, T. Parella, R. Xifra, B. Hedman, K. O. Hodgson, A. Llobet and T. D. P. Stack, *Angew. Chem. Int. Ed.*, 2002, **41**, 2991; (d) B. Yao, D.-X. Wang, Z.-T. Huang, M.-X. Wang, *Chem. Commun.*, 2009, 2899; (e) B. Adinarayana, A. P. Thomas, C. H. Suresh and A. Srinivasan, *Angew. Chem. Int. Ed.*, 2015, **54**, 10478; (f) X. S. Ke, Y. Hong, P. Tu, Q. He, V. M. Lynch, D. Kim and J. L. Sessler, *J. Am. Chem. Soc.*, 2017, **139**, 15232; (g) Z. S. Ghavami, M. R. Anneser, F. Kaiser, P. J. Altmann, B. J. Hofmann, J. F. Schlagintweit, G. Grivani and F. E. Kuhn, *Chem. Sci.*, 2018, **9**, 8307; (h) Y. Liu, S. G. Resch, I. Klawitter, G. E. Cutsail III, S. Demeshko, S. Dechert, F. E. Kühn, S. DeBeer and F. Meyer, *Angew. Chem. Int. Ed.*, 2020, **59**, 5696.
35. The differences in C–X bond strengths are roughly compensated by those in Cu–X bond strengths.
36. Toste *et al.* assessed the possibility for (P,C)-cyclometallated Au(III) complexes to undergo P–C reductive elimination, but no *peri*-bridged naphthyl phosphonium was detected.⁹
37. W. Nakanishi, M. Yamanaka and E. Nakamura, *J. Am. Chem. Soc.*, 2005, **127**, 1446.
38. D. Casanova, J. Cirera, M. Llonell, P. Alemany, D. Avnir and S. Alvarez, *J. Am. Chem. Soc.*, 2004, **126**, 1755.
39. (a) S. Arndt, M. M. Hansmann, F. Rominger, M. Rudolph and A. S. K. Hashmi, *Chem.–Eur. J.*, 2017, **23**, 5429; (b) S. Arndt, J. Borstelmann, R. Eshagh Saatlo, P. W. Antoni, F. Rominger, M. Rudolph, Q. An, Y. Vaynzof and A. S. K. Hashmi, *Chem.–Eur. J.*, 2018, **24**, 7882; (c) T. Kuwabara, T. Kato, K. Takano, S. Kodama, Y. Manabe, N. Tsuchida, K. Takano, Y. Minami, T. Hiyama and Y. Ishii, *Chem. Commun.*, 2018, **54**, 5357; (d) T. Kato, T. Kuwabara, Y. Minami, T. Hiyama and Y. Ishii, *Bull. Chem. Soc. Jpn.*, 2019, **92**, 1131.
40. (a) T. Baumgartner and R. Réau, *Chem. Rev.*, 2006, **106**, 4681; (b) T. Baumgartner, *Acc. Chem. Res.*, 2014, **47**, 1613; (c) M. Hirai, N.

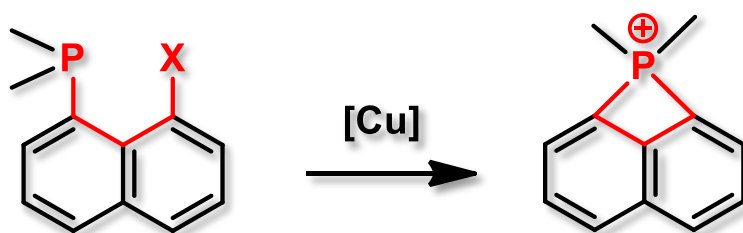
Table of Contents

✓ alkyl, aryl, amino substituents at P

✓ X = I, Br, Cl

✓ amenable to catalysis

(5 min. at rt with 1 mol% Cu)



⚡ 2e Cu(I)/Cu(III) redox sequence (P-coordination, C–X oxidative addition, C–P reductive elimination)

⚡ ring-expansion by insertion of Au(I)